

Uncertainty quantification and out-of-distribution detection using surjective normalizing flows

Simon Dirmeier*

*Swiss Data Science Center
ETH Zurich, Switzerland*

Ye Hong

ETH Zurich, Switzerland

Yanan Xin

ETH Zurich, Switzerland

Fernando Perez-Cruz

*Swiss Data Science Center
ETH Zurich, Switzerland*

Abstract

Reliable quantification of epistemic and aleatoric uncertainty is of crucial importance in applications where models are trained in one environment but applied to multiple different environments, often seen in real-world applications for example, in climate science or mobility analysis. We propose a simple approach using surjective normalizing flows to identify out-of-distribution data sets in deep neural network models that can be computed in a single forward pass. The method builds on recent developments in deep uncertainty quantification and generative modeling with normalizing flows. We apply our method to a synthetic data set that has been simulated using a mechanistic model from the mobility literature and several data sets simulated from interventional distributions induced by soft and atomic interventions on that model, and demonstrate that our method can reliably discern out-of-distribution data from in-distribution data. We compare the surjective flow model to a Dirichlet process mixture model and a bijective flow and find that the surjections are a crucial component to reliably distinguish in-distribution from out-of-distribution data.

1 Introduction

Uncertainty quantification (Lakshminarayanan et al., 2017; Liu et al., 2020; Tagasovska and Lopez-Paz, 2019; Van Amersfoort et al., 2020; Kong et al., 2020; Mukhoti et al., 2023) and distributional robustness (Peters et al., 2016; Meinshausen, 2018; Arjovsky et al., 2019; Heinze-Deml and Meinshausen, 2021; Rothenhäusler et al., 2021) are increasingly being recognized as mandatory features of machine and deep learning methods to find successful applications in industrial or academic settings. For instance, in fields such as climate science or mobility analysis, it is often necessary to be able to train models in one environment, such as the traffic system of a city or the mobility behavior of an individual, and then deploy them in another environment (Xin et al., 2022). Similarly, when a prediction has been made, quantification of predictive uncertainty or confidence levels is often essential for reliable downstream decision-making.

*Correspondence to: simon.dirmeier@sdsc.ethz.ch

In scenarios where decisions need to be taken live, i.e., in location prediction for individual mobility or stock market forecasting in finance, uncertainty estimates are ideally calculated during the evaluation of a data point by a model, e.g., during the same forward pass of a neural network, which forbids computationally intensive approaches (such as Lakshminarayanan et al. (2017) or Tagasovska and Lopez-Paz (2019)). Furthermore, due to the scarcity of data sets in privacy-sensitive disciplines like mobility research which often originate from confidential sources such as user surveys or GPS logs tracking user positions, the necessity arises for a suitable methodology that enables the computation of uncertainty estimates using the same predictive model.

In this work, we build on the work of Mukhoti et al. (2023) and propose an approach to quantify aleatoric and epistemic uncertainty for deep learning models to detect out-of-distribution data. The method first computes epistemic uncertainty estimates using surjective normalizing flows (SNFs; Nielsen et al. (2020); Klein et al. (2021); Dirmeier et al. (2023)) and detects if a data point is out-of-distribution if there is a significant difference to the density estimates of the training data assuming that low density of a data point is an indicator of being out-of-distribution. If the data is in-distribution, aleatoric density estimates can then be computed using the softmax entropy when outputs are discrete or the variance of the prediction when outputs are continuous.

The manuscript is organized as follows. Section 2 introduces the required background and a method that uses SNFs for epistemic uncertainty estimation, specifically, how neural network models can be extended to allow for epistemic uncertainty estimation using SNFs. Section 3 showcases a real-world application from mobility research and evaluates the method in comparison to other density estimators. Section 4 summarizes our findings and discusses future avenues for research.

2 Methods

2.1 Uncertainty quantification

When quantifying uncertainty in scientific applications, it is often required to distinguish *epistemic* from *aleatoric* uncertainty (Hüllermeier and Waegeman, 2021). We denote epistemic uncertainty as uncertainty that stems from insufficient amounts of training data which as a consequence manifests in uncertainty in parameter estimates. Hence, epistemic uncertainty is inversely proportional to the density of data samples and can be used for, e.g., detection of out-of-distribution samples. We denote aleatoric uncertainty as uncertainty of an estimator that is due to, for instance, measurement noise which cannot be reduced by increasing the sample size. Estimates of aleatoric uncertainty are high for ambiguous samples, e.g., if the same feature has been observed for different responses.

2.2 Feature-space regularisation

Mukhoti et al. (2023) demonstrate how neural network models can be used for epistemic and aleatoric uncertainty estimation. Specifically, they propose to regularize the feature-space of the penultimate layer of a neural network and to utilize the outputs up until the pen-ultimate layer (or any layer as a matter of fact) to estimate epistemic uncertainty. To accommodate the feature space for this, they state that it has to be both smooth and sensitive, because feature density alone might be a poor indicator for out-of-distribution (OoD) data and since density estimators might map the data to in-distribution (iD) regions in the feature space. To prevent this feature collapse, Mukhoti et al. (2023) propose subjecting the feature extractor to a bi-Lipschitz constraint, such that

$$K_l d_I(x, x') \leq d_F(h(x), h(x')) \leq K_u d_I(x, x') \quad (1)$$

for all pairs of input data points $x, x' \in \mathcal{X}$, where d_I and d_F are distance measures for input space and feature space, respectively, K_l and K_u are Lipschitz constants, and h is some smooth function. The constraint encourages sensitivity, i.e., preservation of distances in the input space through the lower bound and smoothness, i.e., prevention of too high sensitivity to input variations, through the upper bound. A simple approach to enforce a bi-Lipschitz constraint is via residual connections (He et al., 2016) in a neural

network model, e.g., as given in a conventional transformer architecture (Vaswani et al., 2017), that is trained with spectral normalization (Miyato et al., 2018) (see Mukhoti et al. (2023) for details and references therein).

2.3 Surjective normalizing flows

Vanilla normalizing flows have previously been reported to fail to compute accurate likelihood estimates and detect OoD data (Kirichenko et al., 2020; Dai and Seljak, 2021; Nalisnick et al., 2019; Klein et al., 2021). To alleviate this shortcoming, we make use of a density estimator that projects the data into a lower dimensional manifold via surjective normalizing flows (SNF). We present the derivation thereof in the following section.

Following the SurVAE framework (Nielsen et al., 2020; Klein et al., 2021), we model the log marginal likelihood $p(y)$ of a data point $y \in \mathbb{R}^p$ as

$$\log p(y) = \log p(z) + V(y, z) + E(y, z), \quad z \sim q(z|y) \quad (2)$$

where $p(z)$ is a distribution that can be sampled from efficiently, $q(z|y)$ is some amortized distribution, $V(y, z)$ is denoted as *likelihood contribution* and $E(y, z)$ is denoted as *bound looseness* term. Note that in this representation the random variable z is latent while in the pushforward measure defining a typical normalizing flow, it is not.

Similarly to Klein et al. (2021) and Dirmeier et al. (2023), we partition the data y into two components $y = [y^+, y^-]^T$ (with $y^+ \in \mathbb{R}^q$ and $y^- \in \mathbb{R}^{p-q}$) and define a *generative* (dimensionality-increasing) transformation (i.e., from latent space to data space)

$$y = \begin{bmatrix} y^+ = f_{y^-}(z) \\ y^- \sim p(y^-|z) \end{bmatrix} \quad (3)$$

where $f_{y^-} : \mathbb{R}^q \rightarrow \mathbb{R}^q$ is a conditional normalizing flow (Winkler et al., 2019; Papamakarios et al., 2021), $f_{y^-}^{-1}(y^+)$ its inverse, and $p(y^-|z)$ is a conditional probability density function which we parameterize using a neural network. In the following, we drop the conditioning variable y^- from f_{y^-} for notational clarity.

To connect Equation (2) with the generative transformation of Equation (3), we first observe that by composing a smooth function g with a diffeomorphism f

$$\int \delta(g(y)) f(g(y)) \left| \det \frac{\partial g(y)}{\partial y} \right| dy = \int \delta(u) f(u) du$$

one can conclude that

$$\delta(g(y)) = \delta(y - y_0) \left| \det \frac{\partial g(y)}{\partial y} \right|_{y=y_0}^{-1}$$

where y_0 is the root of $g(y)$ (see also Nielsen et al. (2020); Klein et al. (2021); Dirmeier et al. (2023)). Making use of this derivation we define $g(y) = z - f^{-1}(y^+)$ (which has its root at $y_0 = f(z)$) and

$$q(z|y) = \delta(z - f^{-1}(y^+)) = \delta(y - f(z)) |\det J(y^+)|^{-1}$$

where $J(y^+) = \frac{\partial f^{-1}(y^+)}{\partial y^+}$ is the Jacobian of the bijective inverse transformation. We can now define the likelihood contribution as

$$\begin{aligned}
\mathcal{V}(y, z) &= \mathbb{E}_{q(z|y) \rightarrow \delta(z-f^{-1}(y))} \left[\log \frac{p(y|z)}{q(z|y)} \right] \\
&= \int \delta(z - f^{-1}(y^+)) \log \frac{p(y^- | f^{-1}(y^+))}{\delta(z - f^{-1}(y^+)) |\det J(y^+)|^{-1}} dz \\
&= \int \delta(y^+ - f(z)) |\det J(y^+)|^{-1} \log \frac{p(y^- | z)}{\delta(y^+ - f(z)) |\det J(y^+)|^{-1}} dz \\
&= \int \delta(y^+ - \tilde{y}^+) \log \frac{p(y^- | z)}{\delta(y^T - \tilde{y}^+) |\det J(y^+)|^{-1}} d\tilde{y}^+ \\
&= \log p(y^- | f^{-1}(y^+)) + \log |\det J(y^+)|
\end{aligned}$$

where we used the change of variables $\tilde{y}^+ = f(z)$ yielding $d\tilde{y}^+ = dz |\det J(y^+)|^{-1}$. Transferring this composition to Equation (2):

$$\log p(y) = \log p(z) + \log p(y^- | z) + \log |\det J(y^+)| + E(y, z) \quad (4)$$

As Nielsen et al. (2020) show, the bound looseness term $E(y, z)$ is zero in the case of inference surjections, i.e., the type of dimensionality reducing transformations which we are utilizing in Equation (4), or, more specifically, if the function $f^{-1}(y)$ satisfies the right inverse condition.

Normalizing flows are typically constructed by stacking several flow layers $f = (f_1, \dots, f_K)$ which map a random variable from some easy-to-sample base distribution $z_0 \sim p(z_0)$ to some complex distribution $p(y)$ via the transformations $y = z_K = f_K \circ \dots \circ f_2 \circ f_1(z_0)$. The transformations increase flexibility and expressivity of the target distribution while retaining computational feasibility in case that the Jacobian determinants can be computed efficiently (Rezende and Mohamed, 2015; Papamakarios et al., 2021).

For our model, we facilitate a mixture of dimensionality-retaining bijections and dimensionality-reducing surjections which results in a likelihood that consists of a) some base density term $p(z_0)$, b) Jacobian determinants $\det J_k(\cdot)$ contributed by conventional bijective normalizing flows, and c) Jacobian determinants $\det J_k(\cdot)$ plus conditional densities $p(z_k^- | f_k^{-1}(z_k^+))$ contributed by surjective normalizing flows. Putting these together yields the following likelihood:

$$\begin{aligned}
\log p(y) &= \log p(z_0) + \sum_{k \in \mathcal{K}_b} \log |\det J_k(z_k)| \\
&\quad + \sum_{k \in \mathcal{K}_s} \left(\log p(z_k^- | f_k^{-1}(z_k^+)) + \log |\det J_k(z_k)| \right)
\end{aligned} \quad (5)$$

where \mathcal{K}_b is a set of integers that index bijections and \mathcal{K}_s indexes surjections, respectively and $\det J_k$ are the Jacobian determinants of the inverse mappings f_k^{-1} (c.f. Dirmeier et al. (2023)).

Note that we generally distinguish two types of flows:

- In the case of dimensionality-preserving bijections, the transformations $f_k^{-1}(z_k)$ are unconditional normalizing flows that act on the entire data vector z_k ,
- In the case of dimensionality-reducing surjections, the transformations $f_k^{-1}(z_k^+) := f_{z_k^-}^{-1}(z_k^+)$ are conditional normalizing flows that act on a subset of z_k .

For OoD detection, we use a flow that combines bijective and surjective layers and apply it to estimate the density over the features $y \leftarrow h(x)$ derived from transforming the input data x through a predictive neural network up to some feature layer.

3 Out-of-distribution detection using surjective normalizing flows for mobility research

The following section presents an application of the method in mobility research. We first present the data, then introduce the model and baselines, and finally demonstrate experimental results.

3.1 Data

Following Hong et al. (2023), we use simulated training data for validation of the method, since real data in mobility analysis usually underlies privacy protocols and cannot be shared for research. The training data consists of $N = 800$ discrete location trajectories $\{y_1, \dots, y_N\}$. Each trajectory $y_n = y_n^{1:2000} = (y_n^1, \dots, y_n^{2000})$ consists of 2000 sequential location visits that have been generated through the density transition-EPR (DT-EPR) individual mobility model (Hong et al., 2023). The model combines the density-EPR (d-EPR) (Pappalardo et al., 2015) and individual preferential transition (IPT) (Zhao et al., 2021) mechanisms, both derived from the exploration and preferential return (EPR) framework (Song et al., 2010). For N simulated trajectories, the model begins by simulating an initial location $y_n^{(1)}$ uniformly from a set of available locations $\mathcal{L} = \{l_1, \dots, l_D\}$ where D is the total number of selectable locations. For each successive step, the agent that traverses the locations decides with probability $p_n^{(t+1)} = \rho_n |y_n^{(1:t)}|^{-\gamma_n}$ to explore an unvisited location, where $|y_n^{(1:t)}|$ denotes the number of unique locations in the trajectory up to $y_n^{(t)}$, and ρ_n and γ_n are fixed parameters denoting individual-specific exploration preferences (c.f. Hong et al. (2023) where they are sampled from Gaussians with parameters estimated from observational data). Alternatively, the agent can choose to return to a previously visited location with probability $1 - p_n^{t+1}$. In this case, EPR calculates the probability of selecting a known location as proportional to the visitation frequency of that location.

In order to simulate OoD data and validate their models, Hong et al. (2023) compute interventional distributions by intervening on ρ_n , γ_n and p_n^t by two kinds of interventions:

- They conduct shift interventions on the means of the distributions $\mathbb{P}(\rho)$ and $\mathbb{P}(\gamma)$, i.e., setting $\mathbb{P}(\rho) = \text{Normal}(\mu_\rho, \sigma_\rho^2)$ with $\mu_\rho \in \{0.1, 0.4, 0.7, 0.9\}$ and $\mathbb{P}(\gamma) = \text{Normal}(\mu_\gamma, \sigma_\gamma^2)$ with $\mu_\gamma \in \{0.1, 0.4, 0.7, 0.9\}$.
- They conduct hard interventions on the exploration probabilities p_n^t by setting them to constants $p_n^t \in \{0.1, 0.25, 0.5, 0.75, 0.9\}$.

Hong et al. (2023) simulate "synthetic observational data", i.e., data where the distributions of random variables ρ and γ are parameterized via empirically estimated quantities $\hat{\mu}_\gamma$ and $\hat{\mu}_\rho$, and "synthetic interventional data", i.e., data where random variables are sampled from interventional distributions. They then fit a predictive model on a training set consisting of samples from the observational data set and evaluate the predictor on an observational test set and the interventional data sets.

3.2 Model

We are interested in fitting a density estimator to be able to detect whether the typical trajectory of an individual shows motifs that have not been present in the training data and which would possibly render a prediction of a novel data point to be of low accuracy.

We extend the transformer-based next location prediction model by Hong et al. (2022) to allow for quantification of epistemic and aleatoric uncertainty. In short, Hong et al. (2022) use the encoder architecture of a vanilla transformer model (Vaswani et al., 2017) to learn a predictive model for an individual's next location. The predicted location is represented as a categorical variable, corresponding to specific places like supermarkets or workplaces, and is inferred from the previous location visit history of an individual. Since the model by Hong et al. (2022) is already making use of residual connections, to guarantee a well-behaved feature space of the penultimate layer, one merely needs to spectral-normalize the weights of the attention matrices.

We fit an SNF consisting of 10 normalizing flow layers of which the third and eighth are dimensionality-reducing surjections. All flow layers (also the surjective ones) use masked coupling rational-quadratic neural

spline flows (RQ-NSFs, Dinh et al. (2015; 2017); Durkan et al. (2019); Papamakarios et al. (2021)) as inverse transformations, i.e., from ambient space to embedding space, using 64 bins defined on an interval from -5.0 to 5.0 to fit the boundaries of the data. We use MLP conditioners with 2 hidden layers and 512 nodes per layer to compute the parameters of the RQ-NSFs. The surjective layers require an additional decoder, to parameterize the conditional distribution $p_\phi(y^- | f_{y^-}^{-1}(y^+))$ for which we also use an MLP with 2 hidden layers with 512 nodes each. We use conditional multivariate Gaussians for p_ϕ for which the mean and diagonal of the covariance matrix are computed with the former MLP.

As baselines we use a fully bijective normalizing flow (BNF) that is parameterized as the model described above but does not make use of surjective layers. As a second baseline, we fit a Dirichlet process Gaussian mixture model (DPGMM). We truncate the DPGMM at a maximum of 50 mixture components, such that we can use an optimization-based variational approach for Bayesian inference (see Appendix A for experimental details).

3.3 Experimental results

We fit the three models to the observational training data set of Section 3.1 and evaluate their likelihood estimates on both observational training and test data sets for model selection (Table 1). Despite its complexity, the DPGMM achieves significantly worse likelihood estimates on both train and test sets while the bijective flow (BNF) and the surjective flow (SNF) are relatively similar. We then evaluated the three models on the interventional data sets and computed a likelihood estimate for each data point and model.

	Train set	Test set
DPGMM	147.59	147.52
Bijective normalizing flow	43.33	49.57
Surjective normalizing flow	41.46	47.25

Table 1: Negative log-likelihoods on training set (including validation set) and test set for all three models (lower is better). The flow model that uses surjections achieves more competitive estimates than the other two models.

Graphically, the SNF manages to more reliably detect if a distribution has a distributional shift w.r.t. the training distribution than the other two methods (Figure 1 for SNF and Appendix B for the same visualizations for BNF and DPGMM). In contrast, note the strong overlap between the test data and training data likelihood distributions.

More quantitatively, one can detect if a data set is OoD by, for instance, testing if the means of sub-samples of the feature space likelihood estimates of two data set are significantly separated from each other (see an excerpt in Table 2 and Appendix B for additional results).

	$N = 100$			$N = 200$		
	DPGMM	BNF	SNF	DPGMM	BNF	SNF
Train set	1.00	1.00	1.00	1.00	1.00	1.00
Test set	0.47	0.07	0.09	0.56	8.05^{-3}	1.20^{-2}
Intervention: $p = 0.5$	0.47	3.56^{-11}	9.23^{-25}	0.39	4.52^{-22}	1.43^{-47}
Intervention: $\mu(\gamma) = 0.4$	0.51	2.80^{-9}	2.15^{-21}	0.47	6.40^{-21}	1.36^{-45}
Intervention: $\mu(\rho) = 0.4$	0.49	9.41^{-9}	4.60^{-20}	0.49	2.92^{-19}	1.46^{-44}

Table 2: Two-sample t -tests. Table shows average p -values of 100 repetitions of testing for a difference in means between two randomly sub-sampled feature space likelihood estimates of different data sets. For the first two rows high p -values are better, for the last three rows low p -values are better (see Appendix B for full table and results with Wasserstein distance.)

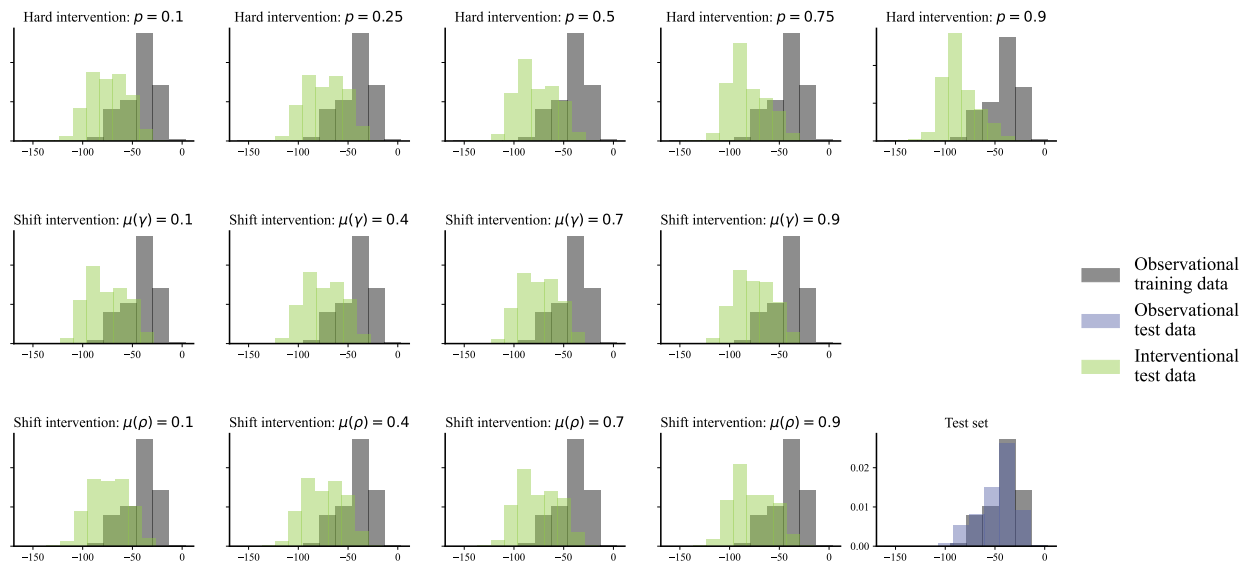


Figure 1: Out-of-distribution detection via density estimation. The SNF manages to reliably detect out-of-distribution data either using simple graphical checks or by conducting statistical tests between pairs of distributions of likelihood estimates. Each of the OoD data sets (green) has a significant distributional shift from the training data set (grey). On the test data set (blue) no significant difference is visible.

4 Conclusion

We introduced a simple method for out-of-distribution detection for data sets from mobility analysis by computing epistemic uncertainty estimates in a deep neural network. The only requirement the method has is to appropriately normalize weights in a neural network architecture during training and to add residual connections to the network structure. We detect OoD samples by comparing the distribution of their epistemic uncertainty estimates to the distribution of uncertainty estimates of the training data and "reject" a sample to be OoD based on a simple statistical significance test. If the test fails to reject the null, we conclude the sample to be iD. We showed that this simple approach can convincingly detect OoD samples on a synthetic observational data set and a multitude of interventional data sets.

Uncertainty quantification (UQ) is of central importance in a wide variety of applications ranging from research in biology to finance to mobility research. Future research in mobility could focus on how ideas from causality, for instance, distributional robustness via invariant prediction or conditional variance penalties (Peters et al., 2016; Heinze-Deml and Meinshausen, 2021) can be integrated into DNN models that already are capable of UQ. Reliable UQ and distributional robustness could pose promising future research avenues to further establish deep learning in application-heavy fields where accurate decision making is crucial.

Acknowledgments and Disclosure of Funding

This work was supported by the Hasler Foundation under the project titled "Interpretable and Robust Machine Learning for Mobility Analysis" (grant number 21041).

References

- Martin Arjovsky, Léon Bottou, Ishaan Gulrajani, and David Lopez-Paz. Invariant risk minimization. *arXiv preprint arXiv:1907.02893*, 2019.
- Igor Babuschkin, Kate Baumli, Alison Bell, Surya Bhupatiraju, Jake Bruce, Peter Buchlovsky, David Budden, Trevor Cai, Aidan Clark, Ivo Danihelka, Antoine Dedieu, Claudio Fantacci, et al. The DeepMind JAX Ecosystem, 2020. URL <http://github.com/deepmind>.
- David M. Blei and Michael I. Jordan. Variational inference for Dirichlet process mixtures. *Bayesian Analysis*, 1(1):121–143, 2006.
- Biwei Dai and Uros Seljak. Sliced iterative normalizing flows. In *ICML Workshop on Invertible Neural Networks, Normalizing Flows, and Explicit Likelihood Models*, 2021.
- Laurent Dinh, David Krueger, and Yoshua Bengio. NICE: non-linear independent components estimation. In *Workshop Track, International Conference on Learning Representations*, 2015.
- Laurent Dinh, Jascha Sohl-Dickstein, and Samy Bengio. Density estimation using real NVP. In *International Conference on Learning Representations*, 2017.
- Simon Dirmeier. Surjectors, 2023. URL <http://github.com/dirmeier/surjectors>.
- Simon Dirmeier, Carlo Albert, and Fernando Perez-Cruz. Simulation-based inference using surjective sequential neural likelihood estimation. *arXiv preprint arXiv:2308.01054*, 2023.
- Conor Durkan, Artur Bekasov, Iain Murray, and George Papamakarios. Neural spline flows. 2019.
- Kaiming He, Xiangyu Zhang, Shaoqing Ren, and Jian Sun. Deep residual learning for image recognition. In *Proceedings of the IEEE conference on computer vision and pattern recognition*, pages 770–778, 2016.
- Christina Heinze-Deml and Nicolai Meinshausen. Conditional variance penalties and domain shift robustness. *Machine Learning*, 110(2):303–348, 2021.
- Matthew D Hoffman, David M Blei, Chong Wang, and John Paisley. Stochastic variational inference. *Journal of Machine Learning Research*, 2013.
- Ye Hong, Henry Martin, and Martin Raubal. How do you go where? improving next location prediction by learning travel mode information using transformers. In *Proceedings of the 30th International Conference on Advances in Geographic Information Systems, SIGSPATIAL '22*, New York, NY, USA, 2022. Association for Computing Machinery.
- Ye Hong, Yanan Xin, Simon Dirmeier, Fernando Perez-Cruz, and Martin Raubal. Revealing behavioral impact on mobility prediction networks through causal interventions. In preparation, 2023.
- Eyke Hüllermeier and Willem Waegeman. Aleatoric and epistemic uncertainty in machine learning: An introduction to concepts and methods. *Machine Learning*, 110:457–506, 2021.
- Hemant Ishwaran and Lancelot F James. Gibbs sampling methods for stick-breaking priors. *Journal of the American statistical Association*, 96(453):161–173, 2001.
- Diederik P. Kingma and Jimmy Ba. Adam: A method for stochastic optimization. In *International Conference on Learning Representations*, 2015.
- Polina Kirichenko, Pavel Izmailov, and Andrew Gordon Wilson. Why normalizing flows fail to detect out-of-distribution data. In *Advances in Neural Information Processing Systems*, 2020.
- Samuel Klein, John A. Raine, Sebastian Pina-Otey, Slava Voloshynovskiy, and Tobias Golling. Funnels: Exact maximum likelihood with dimensionality reduction. In *Workshop on Bayesian Deep Learning, Advances in Neural Information Processing Systems*, 2021.

- Lingkai Kong, Jimeng Sun, and Chao Zhang. SDE-net: Equipping deep neural networks with uncertainty estimates. In *Proceedings of the 37th International Conference on Machine Learning*, 2020.
- Alp Kucukelbir, Dustin Tran, Rajesh Ranganath, Andrew Gelman, and David M Blei. Automatic differentiation variational inference. *Journal of Machine Learning Research*, 2017.
- Balaji Lakshminarayanan, Alexander Pritzel, and Charles Blundell. Simple and scalable predictive uncertainty estimation using deep ensembles. In *Advances in Neural Information Processing Systems*, 2017.
- Jeremiah Liu, Zi Lin, Shreyas Padhy, Dustin Tran, Tania Bedrax Weiss, and Balaji Lakshminarayanan. Simple and principled uncertainty estimation with deterministic deep learning via distance awareness. In *Advances in Neural Information Processing Systems*, 2020.
- Ilya Loshchilov and Frank Hutter. Decoupled weight decay regularization. In *International Conference on Learning Representations*, 2019.
- Nicolai Meinshausen. Causality from a distributional robustness point of view. In *IEEE Data Science Workshop*, pages 6–10, 2018.
- Takeru Miyato, Toshiki Kataoka, Masanori Koyama, and Yuichi Yoshida. Spectral normalization for generative adversarial networks. *arXiv preprint arXiv:1802.05957*, 2018.
- Jishnu Mukhoti, Andreas Kirsch, Joost van Amersfoort, Philip H.S. Torr, and Yarin Gal. Deep deterministic uncertainty: A new simple baseline. In *Proceedings of the IEEE/CVF Conference on Computer Vision and Pattern Recognition*, 2023.
- Eric Nalisnick, Akihiro Matsukawa, Yee Whye Teh, Dilan Gorur, and Balaji Lakshminarayanan. Do deep generative models know what they don’t know? In *International Conference on Learning Representations*, 2019.
- Didrik Nielsen, Priyank Jaini, Emiel Hoogeboom, Ole Winther, and Max Welling. Survae flows: Surjections to bridge the gap between vaes and flows. In *Advances in Neural Information Processing Systems*, 2020.
- George Papamakarios, Eric Nalisnick, Danilo Jimenez Rezende, Shakir Mohamed, and Balaji Lakshminarayanan. Normalizing flows for probabilistic modeling and inference. *The Journal of Machine Learning Research*, 22(1):2617–2680, 2021.
- Luca Pappalardo, Filippo Simini, Salvatore Rinzivillo, Dino Pedreschi, Fosca Giannotti, and Albert-László Barabási. Returners and explorers dichotomy in human mobility. *Nature Communications*, 6(1):8166, 2015.
- Jonas Peters, Peter Bühlmann, and Nicolai Meinshausen. Causal inference by using invariant prediction: identification and confidence intervals. *Journal of the Royal Statistical Society Series B: Statistical Methodology*, 78(5):947–1012, 2016.
- Du Phan, Neeraj Pradhan, and Martin Jankowiak. Composable effects for flexible and accelerated probabilistic programming in numpyro. *arXiv preprint arXiv:1912.11554*, 2019.
- Danilo Rezende and Shakir Mohamed. Variational inference with normalizing flows. In *Proceedings of the 32nd International Conference on Machine Learning*, 2015.
- Dominik Rothenhäusler, Nicolai Meinshausen, Peter Bühlmann, and Jonas Peters. Anchor regression: Heterogeneous data meet causality. *Journal of the Royal Statistical Society Series B: Statistical Methodology*, 83(2):215–246, 2021.
- Chaoming Song, Tal Koren, Pu Wang, and Albert-László Barabási. Modelling the scaling properties of human mobility. *Nature Physics*, 6(10):818–823, 2010.
- Natasa Tagasovska and David Lopez-Paz. Single-model uncertainties for deep learning. In *Advances in Neural Information Processing Systems*, 2019.

- Joost Van Amersfoort, Lewis Smith, Yee Whye Teh, and Yarin Gal. Uncertainty estimation using a single deep deterministic neural network. In *Proceedings of the 37th International Conference on Machine Learning*, 2020.
- Ashish Vaswani, Noam Shazeer, Niki Parmar, Jakob Uszkoreit, Llion Jones, Aidan N Gomez, Łukasz Kaiser, and Illia Polosukhin. Attention is all you need. *Advances in neural information processing systems*, 30, 2017.
- Christina Winkler, Daniel Worrall, Emiel Hoogeboom, and Max Welling. Learning likelihoods with conditional normalizing flows. *arXiv preprint arXiv:1912.00042*, 2019.
- Yanan Xin, Natasa Tagasovska, Fernando Perez-Cruz, and Martin Raubal. Vision paper: causal inference for interpretable and robust machine learning in mobility analysis. In *Proceedings of the 30th International Conference on Advances in Geographic Information Systems*, pages 1–4, 2022.
- Chen Zhao, An Zeng, and Chi Ho Yeung. Characteristics of human mobility patterns revealed by high-frequency cell-phone position data. *EPJ Data Science*, 10(1), 2021.

Appendix A Experimental details

To produce the experimental results in Section 3, we trained a surjective normalizing flow (SNF), a bijective normalizing flow (BNF) as well as a Dirichlet process Gaussian mixture model (DPGMM). We delineate the architectural choices, training procedures, etc. in detail below.

A.1 Normalizing flow models

The SNF uses 10 normalizing flow layers that consist of dimensionality-reducing surjections at the 3rd and 8th layer and dimensionality-preserving bijections everywhere else. The two surjective layers reduce the dimensionality by 25% each meaning that a random subset consisting of 25% of the input vector was randomly chosen to be discarded. In order to not discard information of a relevant dimension it suffices to use bijective layers in front and intermingle them with surjective layers. The architecture of the SNF was chosen somewhat arbitrarily and no hyperparameterization optimization was conducted for a more objective assessment of the model.

Irrespective of the type of layer, all layers use mask coupling with RQ-NSFs (Dinh et al., 2015; 2017; Durkan et al., 2019) as forward transformations f using two-layer MLPs with 512 nodes as conditioners (see Papamakarios et al. (2021) for denotations). RQ-NSFs use half of the input vector as conditioning variables and output parameters for a RQ-spline with 64 bins defined on the interval $[-5, 5]$. The conditional distributions $p(\mathbf{y}^- | \mathbf{z})$ are parameterized as conditional Gaussians using MLPs consisting of two layers with 512 hidden nodes each. All neural networks used `relu` activation functions.

We chose the BNF to be identical in architecture as the SNF with the exception that all layers are dimensionality-preserving. Specifically, all layers are masked coupling layers that use RQ-NSFs and MLP conditioners using two layers of 512 nodes.

We train both models until convergence on mini-batches of size 128 using an AdamW optimizer (Loshchilov and Hutter, 2019) for training with a learning rate of $l = 0.0003$ and otherwise default parameters using the Python library `Optax` (Babuschkin et al., 2020).

Both SNF and BNF are implemented using Python library `Surjectors` (Dirmeier, 2023).

A.2 Mixture model

We fit DPGMMs with truncation at $K \in \{25, 50, 75, 100\}$ components using the following generative model

$$\begin{aligned}
 \alpha &\sim \text{Gamma}(1, 1) \\
 \nu_k &\sim \text{Beta}(1, \alpha) \\
 \boldsymbol{\pi} &\leftarrow \text{break-stick}(\boldsymbol{\nu}) \\
 \boldsymbol{\mu}_k &\sim \text{MvNormal}(\mathbf{0}, \mathbf{1}) \\
 \sigma_{kp} &\sim \text{HalfNormal}(1) \\
 \boldsymbol{\Sigma}_k &\leftarrow \text{diag}(\boldsymbol{\sigma}_k^2) \\
 y_i &\sim \sum_{k=1}^K \pi_k \cdot \text{MvNormal}(\boldsymbol{\mu}_k, \boldsymbol{\Sigma}_k)
 \end{aligned}$$

where we characterize the DP using the (truncated) stick-breaking construction (Ishwaran and James, 2001; Blei and Jordan, 2006).

$$\pi_i(\boldsymbol{\nu}) = \nu_i \prod_{j=1}^{i-1} (1 - \nu_j)$$

	$N = 100$			$N = 200$		
	DPGMM	BNF	SNF	DPGMM	BNF	SNF
Train set	1.00	1.00	1.00	1.00	1.00	1.00
Test set	0.47	0.07	0.09	0.56	8.05^{-03}	1.20^{-02}
Hard intervention: $p = 0.1$	0.50	2.73^{-8}	1.84^{-19}	0.49	6.40^{-20}	1.77^{-46}
Hard intervention: $p = 0.25$	0.51	2.90^{-8}	7.03^{-19}	0.53	8.65^{-15}	1.42^{-37}
Hard intervention: $p = 0.5$	0.47	3.56^{-11}	9.23^{-25}	0.39	4.52^{-22}	1.43^{-47}
Hard intervention: $p = 0.75$	0.44	1.61^{-16}	2.00^{-30}	0.37	3.22^{-36}	1.48^{-63}
Hard intervention: $p = 0.9$	0.35	3.95^{-21}	5.66^{-37}	0.294	2.03^{-45}	8.66^{-78}
Shift intervention: $\mu(\gamma) = 0.1$	0.47	4.00^{-11}	3.82^{-24}	0.46	2.34^{-21}	9.17^{-48}
Shift intervention: $\mu(\gamma) = 0.4$	0.51	2.80^{-9}	2.15^{-21}	0.47	6.40^{-21}	1.36^{-45}
Shift intervention: $\mu(\gamma) = 0.7$	0.53	9.00^{-10}	1.44^{-23}	0.49	5.15^{-21}	7.80^{-48}
Shift intervention: $\mu(\gamma) = 0.9$	0.50	4.70^{-12}	1.49^{-25}	0.44	1.14^{-20}	5.41^{-46}
Shift intervention: $\mu(\rho) = 0.1$	0.54	8.43^{-9}	8.30^{-22}	0.53	2.11^{-19}	3.91^{-46}
Shift intervention: $\mu(\rho) = 0.4$	0.49	9.41^{-9}	4.60^{-20}	0.49	2.92^{-19}	1.46^{-44}
Shift intervention: $\mu(\rho) = 0.7$	0.49	4.23^{-10}	4.22^{-22}	0.48	1.04^{-21}	7.44^{-46}
Shift intervention: $\mu(\rho) = 0.9$	0.48	1.32^{-10}	1.38^{-21}	0.42	1.14^{-25}	1.27^{-49}

Table 3: Two-sample t -tests. Table shows average p -values of 100 repetitions of testing for a difference in means between two randomly sub-sampled feature space likelihood estimates of different data sets. For the first two rows high p -values are better, for the last rows low p -values are better.

which is amendable to optimization using automatic-differentiation variational inference (Hoffman et al., 2013; Kucukelbir et al., 2017) which we conduct using the probabilistic programming language NumPyro (Phan et al., 2019) using an Adam optimizer with learning rate $lr = 0.003$ (Kingma and Ba, 2015).

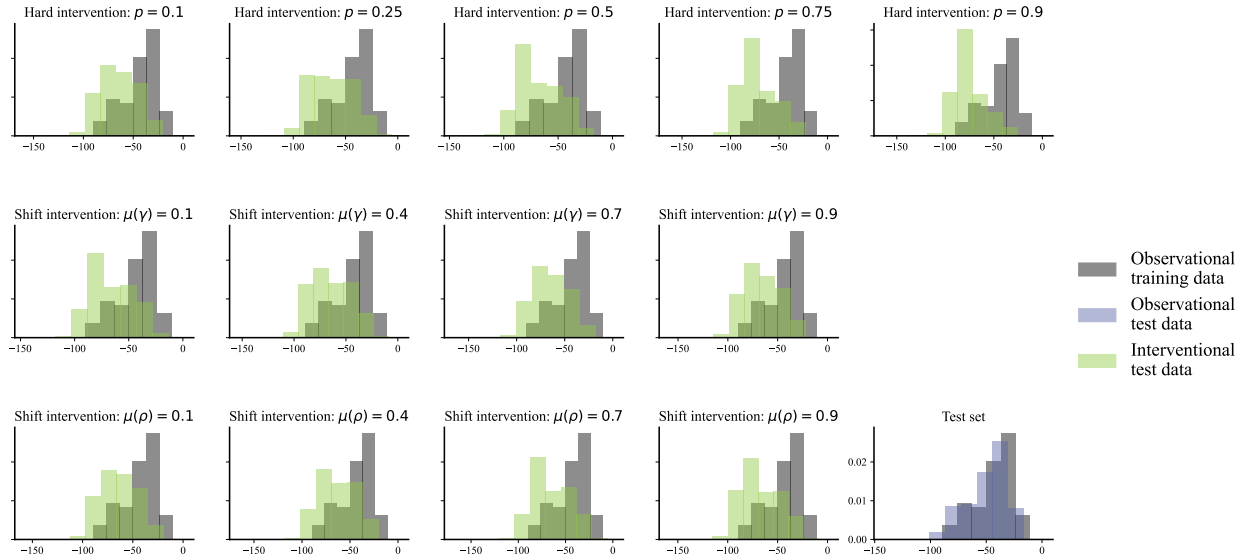
We compute the likelihood of the test data \mathbf{y}^* via integrating over the posterior of the variables $\boldsymbol{\theta} = (\pi_k, \boldsymbol{\mu}_k, \boldsymbol{\Sigma}_k)$: $\int p(\mathbf{y}^*|\boldsymbol{\theta})p(\boldsymbol{\theta}|\mathbf{y})d\boldsymbol{\theta}$.

Appendix B Additional experimental results

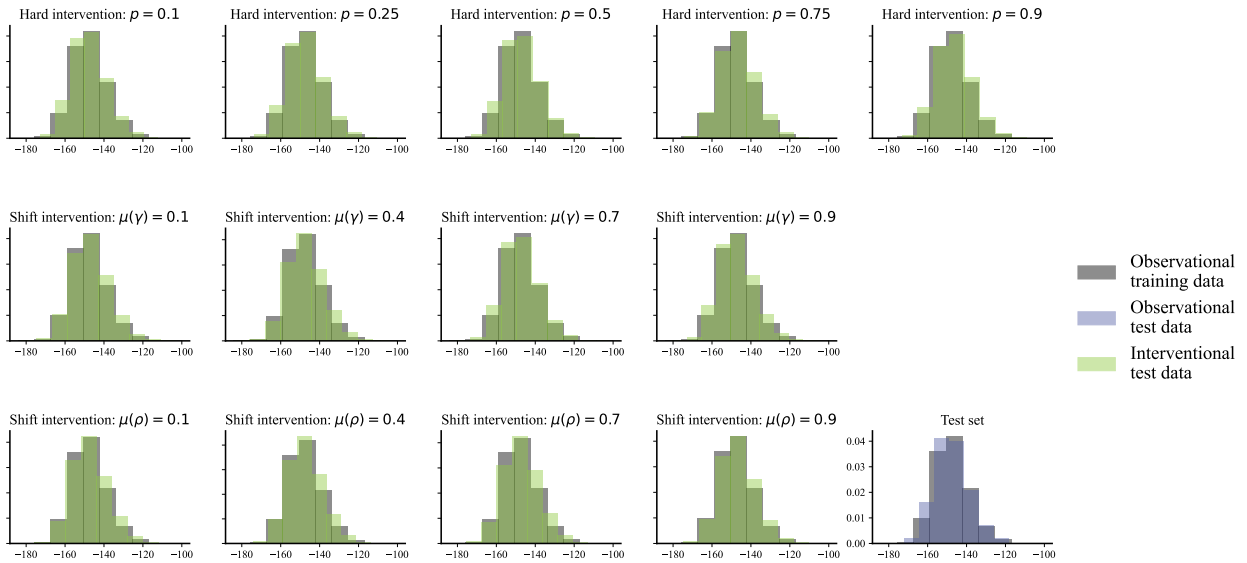
B.1 Source code

Source code to fit a custom density estimator for OoD detection can be found on GitHub.

B.2 Additional figures



(a) Out-of-distribution detection BNF. We visualize the empirical density estimates when using a BNF as a density estimator (compare Figure 1).



(b) Out-of-distribution detection DPGMM. We visualize the empirical density estimates when using a DPGMM as a density estimator (compare Figure 1).

	$N = 100$			$N = 200$		
	DPGMM	BNF	SNF	DPGMM	BNF	SNF
Train set	0.00	0.00	0.00	0.00	0.00	0.00
Test set	1.62	6.58	6.04	1.07	6.56	6.03
Hard intervention: $p = 0.1$	1.53	20.88	32.79	1.09	21.10	33.08
Hard intervention: $p = 0.25$	1.63	19.80	31.31	1.10	20.05	31.80
Hard intervention: $p = 0.5$	1.69	23.94	35.70	1.29	24.08	35.83
Hard intervention: $p = 0.75$	1.82	28.54	40.60	1.36	28.46	40.32
Hard intervention: $p = 0.9$	2.04	32.35	44.44	1.59	32.35	44.54
Shift intervention: $\mu(\gamma) = 0.1$	1.75	22.45	34.35	1.21	22.72	34.59
Shift intervention: $\mu(\gamma) = 0.4$	1.64	21.08	33.13	1.18	21.32	33.26
Shift intervention: $\mu(\gamma) = 0.7$	1.53	21.59	33.38	1.15	21.53	33.47
Shift intervention: $\mu(\gamma) = 0.9$	1.59	22.62	34.49	1.23	22.65	34.48
Shift intervention: $\mu(\rho) = 0.1$	1.61	20.40	32.39	1.10	20.89	32.71
Shift intervention: $\mu(\rho) = 0.4$	1.61	20.54	32.32	1.12	20.62	32.25
Shift intervention: $\mu(\rho) = 0.7$	1.63	22.48	34.33	1.17	22.37	34.16
Shift intervention: $\mu(\rho) = 0.9$	1.72	23.81	35.60	1.28	24.20	36.13

Table 4: Two-sample $1d$ -Wasserstein distances. Table shows average Wasserstein distances of 100 repetitions between two randomly sub-sampled feature space likelihood estimates of different data sets. For the first two rows high low distances are better, for the last rows high distances are better.